Characterization of a Charged Biomimetic Lipid Membrane for Unique Antifouling Effects against Clinically Relevant Matrices in Biosensing

Daniel D. Stuart, Caleb D. Pike, Alexander S. Malinick and Quan Cheng*

Department of Chemistry
University of California, Riverside, CA 92521

*Corresponding author: Quan Cheng
Tel: (951) 827-2702
Fax: (951) 827-4713
Email: quan.cheng@ucr.edu

ABSTRACT:

Clinically relevant matrices such as human blood and serum can cause substantial interference in biosensing measurements, severely compromising effectiveness of the sensors. We report the characterization of a positively charged lipid membrane that has demonstrated unique features to suppress nonspecific signal for antifouling effects by using SPR, fluorescence recovery after photobleaching (FRAP), and MALDI-TOF-MS. The ethyl phosphocholine (EPC) lipid membrane proved to be exceptionally effective at reducing irreversible interactions from human serum on a Protein A surface. The membrane formation conditions and their effects on membrane fluidity and mobility were characterized for understanding the antifouling functions when various capture molecules were immobilized. Specifically, EPC lipid membranes on a Protein A substrate appear to exbibit a strong interaction, likely through the electrostatic effect with the negatively charged proteins that resulted in a stable hydration layer. The strong interaction also limited lipid mobility, contributing to a robust, protective interface that remained undamaged in undiluted serum. Tailoring a surface with antifouling lipid membranes allows for a range of biosensing applications in highly complex biological media.

Keywords: Antifouling, Lipid Membranes, Surface Plasmon Resonance, Biomimetic, Serum, Biosensing

INTRODUCTION:

Analysis of biomarkers in complex biological media is an important step for tracking human disease states, drug effectiveness, toxicant exposure, and overall patient health. A number of biosensors have been developed for this important application[1, 2], but many have encountered a considerable technical issue, which is to effectively separate signals of the biomarkers of interest from the signal caused by nonspecific interactions by other biological molecules. Many biological molecules in clinically relevant fluids (blood, saliva, cerebrospinal fluid, and nasopharyngeal swabs) notoriously and nonspecifically adhere to sensor surfaces and convolute sensor signals.[3] To curtail this problem, extensive research efforts have been spent on the development of surfaces and methodologies to block, remove or correct for nonspecific interactions.[4-8] These methods generally rely on surface blocking with thiol self-assembled monolayers (SAMs)[9, 10], polymer surfaces[11], DNA structures[12], or peptides[13, 14]. Lipids, another subset of biological molecules, have also been found to be a reliable method for blocking nonspecific adsorption as they are a major component of inherently antifouling cell membranes.[4, 15, 16] The ability of lipids to self-assemble into bilayers allow them to be easily presented on sensor surfaces[17] and can be utilized to mimic cell surface environments in addition to the adsorption-blocking capabilities.[18] However, these surfaces are considerably underutilized due to stability issues despite their inherent benefits. New designs towards more effective antifouling and a better understanding of the process behind antifouling effects are clearly needed.

A variety of lipids have been utilized for constructing the sensing interface that improved the performance of the analysis in serum[4] and blood[19,20]. Zwitterionic polymers have been broadly used due to overall neutral charge with a strong hydration effect that is often considered an advantage in antifouling.[21, 22] As such, zwitterionic lipids have been viewed as an ideal starting point for lipid membrane-based antifouling.[19] However, the role charged lipids play in nonspecific interactions appears to be complex. On certain surfaces, zwitterionic lipid bilayer are found to be far less effective.[4] On the other hand, charged lipids have not been fully explored for their potential in antifouling, despite many of which play important roles in cellular membranes.[23-25] Until recently there were no reports using a charged lipid membrane interface for sensing application in biological matrices where reduced background was noticed. However, we recently demonstrated that positively charged ethyl phosphocholine (EPC) lipid membrane showed better antifouling property than zwitterionic lipids in protein detection on a Protein A

substrate in undiluted serum.[4] Protein A was used for its capacity to bind to antibodies in their Fc region, thus presenting the antibodies in a desired orientation on the sensor surface to capture target proteins. Nevertheless, the process behind the antifouling properties of EPC/Protein A and the EPC lipid system was not fully understood.

In this work, we further characterized the positively charged EPC lipid membrane and sought to identify key factors that determined the antifouling behavior in human serum (Scheme 1). A number of surface techniques, including surface plasmon resonance (SPR), fluorescence recovery after photobleaching (FRAP), and MALDI-TOF-MS, were utilized to provide molecular level understanding of the membrane properties, especially those on a Protein A substrate. SPR has been used by us and others to study lipid membrane surfaces and allows for real time analysis of membrane formation and interactions at the membrane surface.[4, 26] FRAP is a commonly used method to measure lipid mobility which is an important parameter of lipid bilayers.[27] The molecular identity of species present at SPR surfaces can be difficult to obtain, and MALDI-TOF-MS solves this limitation effectively. MALDI has been broadly used for this purpose in SPR studies due to the ease of chip transfer and the complementary nature of their surface-based analyses.[28] Zwitterionic POPC lipid, a standard lipid molecule broadly used for antifouling purposes, will be employed for comparison. POPC demonstrates effective antifouling capabilities on surfaces of glass and calcinated Au substrates[15], but was observed to function less effectively on a protein-modified surface. Negatively charged lipids proved difficult to even form into a membrane system on Protein A and silica surfaces, let alone the surface antifouling effect. This study probes into possible mechanisms behind the antifouling properties of EPC lipids, providing potential guidance for construction and utilizing of lipid membranes to suppress nonspecific signals in biosensor research.

EXPERIMENTAL:

Reagents. Super dihydrobenzoic acid (sDHB), acetonitrile (ACN), and trifluoroacetic acid (TFA) with purity (>99%) were purchased from Sigma Aldrich. Premium Plain BK-7 glass microscope slides and phosphate buffered saline (PBS) concentrate were purchased from Fisher Scientific. Thiolated recombinant Protein A was purchased from ProteinMods. Ultrapure water (>18 MΩ cm-1) was acquired from a Barnstead E-Pure water purification system.

Lipid Vesicle Preparation. Stocks of 1-palmitoyl-2-oleoyl-sn-glycero-3-phosphocholine (POPC; 5 mg mL^{-1}), 1,2-dioleoyl-sn-glycero-3-ethylphosphocholine (EPC; 5 mg mL^{-1}), 1-palmitoyl-2-oleoyl-sn-glycero-3-phospho-(1'-rac-glycerol) (POPG; 5 mg mL^{-1}), and 1,2-dipalmitoyl-sn-glycero-3-phosphoethanolamine-N-(7-nitro-2-1,3-benzoxadiazol-4-yl) (ammonium salt) (NBD-PE; 5 mg mL^{-1}) were obtained from Avanti Polar Lipids, then diluted in chloroform to the designated concentration and stored at −80 °C. For lipid vesicle formation, lipid stock solution was aliquoted into glass vials and dried under nitrogen forming thin lipid films which were further dried overnight in a vacuum desiccator. The dried lipids were resuspended in 1× PBS (10 mM Na_2HPO_4, 1.8 mM KH_2PO_4, 137 mM NaCl, 2.7 mM KCL, pH 7.4) to a final concentration of 1 mg mL^{-1} (above critical micelle concentration), followed by vigorous vortexing and bath sonication for 30 min to induce vesicle formation. The resulting lipid vesicles were then extruded through a polycarbonate filter (Whatman, 100 nm) to produce small unilamellar vesicles of uniform 100nm size. All lipid vesicle suspensions were stored at 4 °C and used within 1 week of preparation to ensure consistent vesicle structure and resulting membrane formation.

Fabrication of Sensor Chips. Gold SPR chips were fabricated from BK-7 glass slides based on a previously published procedure with modification.[29] In short, glass slides were cleaned with boiling piranha solution (3:1 H_2SO_4 and 30% H_2O_2; **Caution!**) for 2 h and then rinsed with equal amounts water and absolute ethanol before drying under nitrogen. A 2-nm layer of chromium (0.5 Å s^{-1}) followed by a 48 nm layer of gold (1.0 Å s^{-1}) was deposited onto the glass slides using an electron-beam physical vapor deposition system (Temescal, Berkeley, CA) at or below 5×10^{-6} Torr. Silicated chips were fabricated through additional deposition of approximately 1-3 nm of SiO_2 via plasma enhanced chemical vapor deposition using a Unaxis Plasmatherm 790 system (Santa Clara, CA), onto previously described gold chips. All sensor chips were fabricated in a Class 100/1000 cleanroom facility (UCR Center for Nanoscale Science & Engineering). Gold sensor chips were chemically functionalized following previously disclosed methods.[4] In short, 10 μg mL^{-1} thiolated Protein A and 1mM 3-mercapto-1-propanol were incubated on gold sensor chips for 2h and 1 h, respectively. Chips were then rinsed with ultrapure water, dried under nitrogen, and stored at 4 °C prior to SPR analysis.

SPR Analysis of Membrane Formation and Antifouling Properties. SPR analysis was conducted on a NanoSPR6 instrument (NanoSPR, Addison, IL, USA) using 1× PBS as the running buffer with a flow rate of 5 mL h^{-1} (ca. 83 μL min^{-1}). Lipid deposition was carried out by injection of 1 mg mL^{-1} of 100 nm lipid vesicles, which were allowed to self-assemble into bilayers over 30 minutes of stopped flow. Following a 30 min rinse with 1× PBS, undiluted human serum was introduced and allowed to interact with the surface for 30 min with flow set to zero, followed by a final 30 min rinse with PBS.

Fluorescence Recovery after Photobleaching. Fluorescence microscopy and bleaching images were generated on an inverted Leica TCS SP5 II confocal microscope (Leica Microsystems, Buffalo Point, IL, USA). NBD-PE lipids (2% in molar ratio) were incorporated into vesicle preparation methods to enable fluorescent visualization of lipid membranes. For fluorescent imaging an argon laser at the wavelength of 488nm was utilized to excite NBD lipid. Fluorescent emission between 500 and 600 nm was detected using a hybrid detector (HyD). Images were obtained via 3 line averaging and further 3 image averaging. FRAP images were obtained without image averaging and with laser power increased to 100% for one second bleaching. Photobleaching and monitoring of fluorescence recovery within defined regions of interest were performed using the LAS AF software package (Leica). Images were processed using ImageJ with the Fiji package and analyzed using open-source software simFRAP (available through http://imagej.nih.gov/ij/plugins/sim-frap/index.html).[30] Mobile fractions (ß) and diffusion coefficients (D) were calculated using previously demonstrated methods.[31, 32]

Matrix Assisted Laser Desorption Ionization. Mass profiles of membrane systems before and after serum interaction were obtained with a reflectron AB-Sciex 5800 MALDI-TOF instrument operating in positive ion mode. An individual spectra is represented by m/z values versus intensity (au) obtained by an average of 200 shots collected from a small area of the chip. To enable spectra acquisition post SPR analysis air was slowly injected into the flow system to dry the chip surface leaving behind surface bound materials before removal of the chip from the SPR instrument and matrix deposition prior to MALDI analysis.

RESULTS AND DISCUSSION:

Formation of Lipid Membranes on Functional Surfaces. Fused EPC lipid membrane on a Protein A substrate has been identified as a unique platform to enable antibody capture and detection in serum that suppresses nonspecific interactions, improves detection limits and deconvolutes data.[4] The underlying principle of the antifouling function with a positively charged membrane, however, remains unclear. In this work we further characterized the EPC system under various conditions, aiming to elucidate how charged lipid membranes enable improvements, both in antifouling and specific sensing, on Protein A supports. We first tested the effect of varied surface charges on the formation of lipid membranes and compared membrane formation on different surfaces using SPR. The test chips were coated with Protein A (10 μg mL^{-1}), followed by passivation with MPO (1mM). Lipid vesicles of negatively charged POPG, positively charge EPC and zwitterionic POPC (Figure 1A) were introduced into the flow cell for membrane self-assembly.[4] Only positively charged EPC lipids appeared to self-assemble on the Protein A substrate, while POPG and POPC lipid vesicles did not register any binding or fusion (Figure 1C). The observed response patterns seemed unique, and a possible scenario of electrostatic repulsion or minimal vesicle adhesion without rupture could be proposed as the cause.[33]

It is known that Protein A is negatively charged in the buffer condition used here (pH 7.4) from a theoretical isoelectronic point of 5.4.[34] However, the complete shutoff of POPC lipid vesicles is puzzling. The role of Protein A on membrane formation appears to be more complex than initially believed. We further tested vesicle fusion using silica substrates as they are known to promote self-assembly of lipid membranes.[17] For this comparison work, we utilized calcinated gold chips with SPR that were previously developed in our lab.[35] With SPR the binding and fusion of lipid vesicles to the sensor surface could be measured as angular shifts caused by changes in refractive index at the sensor surface, with greater shifts attributable to greater amounts of bound material. Figure 1B shows that POPC and EPC quickly formed robust membranes, which agrees well with literature reports.[36] There were some differences in signal magnitude for different vesicles, with EPC lipid vesicles producing a greater angular shift ($\Delta\theta$ = 0.445°) as compared to POPC vesicles ($\Delta\theta$ = 0.350°) (Figure 1B).

Negatively charged POPG vesicles, however, showed minimal interaction with the calcinated substrates ($\Delta\theta$ = 0.024°), likely due to the negative charge of the silica surface in PBS buffer.[37] The observation of positively charged EPC showing favorable interaction with the silica

surface provides some explanation about the difference in signal between EPC and POPC lipids. Strong charge interactions constrain EPC lipid vesicles closer to the sensor surface, enabling a better packing of the EPC membrane. Zwitterionic POPC also demonstrates prolific membrane formation on a silica surface, as have been broadly reported.[38-40] The signal was slightly smaller than EPC, indicative of a less tightly packed structure. It is interesting to note that EPC lipids formed on a Protein A substrate had a higher angular shift than on the silica surface ($\Delta\theta$ = 0.576°), providing further evidence that EPC lipids interact more strongly with the charged Protein A substrates and the impact of charge density and lipid packaging density play important roles in the interaction and resulting antifouling properties.

Fluorescence microscopy was utilized to characterize the distribution and mobility of EPC and POPC lipid species on the two surfaces. Glass slides and Protein A coated gold chips were prepared in a similar fashion and fitted into a PMDS housing to provide a defined area for vesicle incubation. 2 mol % of NBD-PE was incorporated into the membrane systems to enable fluorescent visualization. To address the concern of fluorescent quenching on gold surfaces, which could limit fluorescent imaging on these chips[41], we first tested if fluorescent signal was impacted on the 50 nm thick gold substrates. We didn't observe any substantial quenching or signal complications, likely thanks to the increased distance of the fluorophores from the gold substrate, separated by the Protein A scaffold (data not shown). Distance from the gold has been shown to be an important component of gold quenching mechanisms.[41] EPC and POPC distribution on the silica substrate was uniform with no visible, uncovered areas. For comparison, EPC coverage on the Protein A surface was complete while POPC was only sparsely distributed (data not shown).

Mobility measurement by FRAP further separated these lipid surfaces where significant differences were observed. EPC lipids on the Protein A sensor presented a complete lack of lateral mobility while both EPC and POPC demonstrated decent mobility on the silica surface. POPC lipids showed a measured mobility with D = 2.87 ± 0.25 $\mu m^2/s$, which is consistent with literature reports,[42] whereas EPC had rather reduced mobility values (1.89 ± 0.19 $\mu m^2/s$) (Figure S1). These differences fit well into a charge-based model in which increased electrostatic charge plays a larger role in positively charged EPC with negatively charged silica as compared to zwitterionic POPC lipids thus limiting lipid lateral movement. As POPC vesicles did not fuse onto the Protein A surface, they therefore did not have measurable diffusivity.

Antifouling Properties of Lipid Bilayers. We then used SPR to quantify the changes upon injection of serum to further characterize the antifouling properties of the lipid membranes. Lipid membranes of POPC, EPC, and POPG were formulated as previously described, and were allowed to interact with serum over a 30-minute period before a final rinse step was performed. Figure 2 (C)(D) shows the SPR signals as a result of the bulk refractive index change at the interface brought about by the binding of biological molecules in serum. After PBS washing, the bulk signal changed and was replaced in the sensorgram by remaining molecules attributing to the non-specific binding, which was used for quantifying the extent of surface fouling. For membranes where the SPR signal returned to pre-serum levels, the outcome indicated that little to no irreversible interactions between the surface and molecules in serum occurred during the incubation and the surface would be thus deemed "effective antifouling". This property was clearly observed for EPC on a Protein A surface and POPC on a silica surface. Other surfaces were observed with substantial remaining signal, which were designated high levels of surface fouling, as seen on the bare chip surfaces and those where lipid membranes did not form.

From SPR surface fouling tests, it is apparent that the Protein A sensor has much more nonspecific interactions than silica substrates (Figure 2E&F). The angular shift remained high after rinse (0.630 ± 0.042°) while the silica substrate only showed half of the shift (0.383 ± 0.045°). This nearly two-fold higher nonspecific signal demonstrates that nonspecific interactions can severely impair biosensor performance if surface fouling is not effectively addressed. From the results, two substrates with lipid membrane coating stand out: EPC lipids on the Protein A surface (Figure 2E) and POPC lipids on the silica substrate (Figure 2F), with observed angular shifts at -0.095 ± 0.048° and 0.014 ± 0.009°, respectively. The negative values on the Protein A/EPC surface raised questions about whether the lipids were displaced by or exchanged with serum proteins. Therefore, we employed a series of methods including fluorescent microscopy, FRAP and mass spectrometry to further investigate the surface properties after serum incubation.

It should be mentioned that the POPC and POPG membranes tested in this work showed considerable nonspecific signal, suggesting that a variety of non-specific interactions had occurred between the sensor substrate and biomolecules in serum. Thus, these surfaces would perform poorly for sensor development. However, there is some variation in the extent of fouling

among those ineffective surfaces, which may provide some clue on how these surfaces could be improved. POPC lipid vesicles on the Protein A surface, previously mentioned only sparsely adhered to the sensor surface, did provide a lower nonspecific adsorption, with remaining angular shift observed at 0.465 ± 0.130°, which is ~27% less than the noncoated, bare Protein A sensor. The relatively high values match the observed surface condition as only being limitedly covered, suggesting that should mechanisms to induce POPC vesicle fusion on this surface be developed it could prove to be effectively antifouling, as even the small amount of POPC lipids attached were able to reduce the signal from nonspecific interactions. Several approaches such as amphipathic peptide induced fusion[43] and solvent/buffer assisted fusion[44] have been shown to promote lipid coverage. Their effectiveness for POPC on Protein A surface remains to be tested. Nevertheless, we showed lipid membranes can be formulated to match surface property of the sensor chips for optimal antifouling results. The highly effective Protein A/EPC system presents the most promising surface in antifouling and thus was further investigated to understand what key factors are behind the antifouling properties.

Probing Factors behind EPC Antifouling Properties on Protein A Surface. As previously mentioned, a reduction in signal following serum incubation on the EPC coated Protein A surface was observed. To confirm that EPC lipid membranes remained intact and were not damaged by serum we performed fluorescent microscopic studies to evaluate surface coverage and mobility before and after serum introduction. Each measurement was referenced against a control region containing the same lipid system without the addition of fluorescent lipids. Protein A/EPC chips with 2% NBD-PE were prepared as with the SPR experiments and were characterized for lipid coverage and bleaching/recovery tracking (Figure 3A&B). Chips without serum incubation were compared to identify differences in coverage and density. Fluorescence of Figure 3D shows that serum incubation resulted in a small decrease in fluorescent intensity, likely due to the extra washing steps associated with the removal steps. However, the difference was small and complete fluorescent coverage was observed across the whole lipid membrane surface, indicating the membrane remained intact following serum incubation. The result matches well with SPR study that exhibited a small signal reduction following serum wash off. We speculate the minor signal loss is due to small amounts of lipid debris separating from the surface while the overall membrane structure remains intact. The high stability of the EPC

membrane on Protein A in serum is one important factor in abrogating serum fouling. Control study with bare Protein A surface indicated that no fluorescent signal was observed from Protein A or serum, confirming that the lipid membranes were the only source of fluorescent signal (Figure 3C&D). FRAP analysis was performed on both substrates and similar non-recovery behavior was observed (Figure 4). The fractional recovery curve remained flat, suggesting very little lateral diffusion on these surfaces and no change in membrane properties following serum introduction.

MALDI-MS characterization of the sensor chips following SPR analysis was performed to identify molecular constituents on the surface. Sensor chips were removed from the SPR instrument, dried, and spotted with MALDI matrix (sDHB). As can be seen in Figure 5, no peaks for the Protein A chip were detected above noise beyond 3000 m/z; with vast majority appearing below 1200 m/z. Protein A is a 49-kDa protein and a large scan beyond 50,000 m/z was performed to determine if whole Protein A would be ionized. However, no such peaks were observed, likely due to covalent linkage of Protein A to the sensor surface and MALDI's soft ionization meaning fragmentation is rare.[45] Below 1200 m/z range, there was clear signals for EPC lipids, identified at 789.01 m/z appearing in both samples. This matches with MALDI spectra for an EPC standard (Figure S2). As such, it is clear that EPC lipids remained on the sensor surface in large quantity following serum incubation. The overlapped spectra also exhibit no peaks only seen in the serum treated sample, additionally demonstrating that no serum molecules remain nonspecifically interacted with the sensor surface. From the MALDI-MS results, EPC lipid membranes appeared to be very stable on the Protein A surface, exhibiting exceptionally effective function at reducing serum fouling on the surface.

Understanding Potential Antifouling Processes of the EPC Protein A Surface. With the antifouling effectiveness of EPC lipid membranes on Protein A scaffolds successfully being demonstrated we turned towards understanding how and why this surface was effective. Previous results indicated that strong interaction between the sensor surface and EPC lipids occurs, generating robust SPR signal with diminishing lateral mobility. But how these interactions resulted in such an antifouling surface was elusive. We first tested the effect of Protein A density on lipid membrane formation and property. Sensor chips prepared with varied Protein A concentrations (1 μg mL^{-1}, 100 ng mL^{-1}, and 1 ng mL^{-1}) in the incubation step were fabricated,

yielding surfaces with a more disperse protein distribution. SPR sensorgrams demonstrated significant differences in membrane formation and antifouling properties. Lowering Protein A concentration led to a loss of function towards nonspecific interactions from serum by the EPC lipids on top of it (Figure S3). On the other hand, POPC membranes started to steadily form on the sensor surface when concentration of Protein A was decreased.

FRAP analysis of EPC membranes formed on these Protein A surfaces provided additional information about the mobility changes in the membrane. As Protein A concentration increased, a decrease in lipid fluidity was observed, with a complete loss of fluidity observed at 10 μg mL^{-1} (Figure 6). Diffusion coefficient measurement indicates the value decreased by 0.08 $\mu m^2/s$ with concentration increased from 1 to 100 ng mL^{-1}, while a loss of 0.12 $\mu m^2/s$ was determined with the concentration increased from 100 ng mL^{-1} to 1 μg mL^{-1}. Clearly the density of Protein A has a large impact on the formation and the mobility of EPC lipids. We speculate that the low mobility of the EPC membrane may be a necessary factor for the surface to remain stable in serum and act as an effective antifouling substrate.

While surface charge has been established to play a role in the formation of EPC membrane and the antifouling properties, another speculated factor could be the hydration layer formed above the lipid surface. The highly charged gel phase of EPC lipid has a strong coupling with the interfacial hydration layer, increasing the energy required for proteins to undergo conformational changes that would lead to irreversible nonspecific binding.[46] The scenario is similar to an aluminum oxide surface that proves to be highly antifouling[47] due to the thicker hydration layer, [48] resulting from strong coupling between the positively charged aluminum oxide and water layer.[49] Furthermore, the EPC terminal phosphocholine group likely plays a large role due to its ability to form multiple hydrogen bonds to water molecules.[50] Recently phosphate groups, despite lacking zwitterionic properties, have been demonstrated to impart antifouling properties due to their strong hydrophilicity.[51] Indicating that zwitterionic charge is not necessary for antifouling and that the hydrophilicity or hydrophobicity of a substrate likely plays a large role in antifouling effectiveness. This explains why EPC antifouling properties are completely lost upon decreasing Protein A concentration and the EPC bilayer becomes more fluid and dispersed.

CONCLUSION:

We have reported the characterization of membrane formation of differently charged lipids, including POPC, EPC, and POPG on Protein A surface and their respective antifouling properties. POPC and EPC membranes were found to effectively form antifouling substrates against whole human serum. Various formation conditions have been explored and the importance of charge interactions with the underlying surface is found to play a pivotal role in whether antifouling properties are observed. Notably POPC on a silica surface and EPC on a Protein A surface demonstrate highly effective antifouling properties. EPC lipid surfaces were confirmed to remain intact and can deter serum molecules from irreversibly adhering to the surface through robust bilayer formation, electrical repulsion, and formation of a hydration layer. At higher Protein A concentrations EPC lipid membranes are robust therefore antifouling relies on a strong interaction between Protein A and EPC that severely limits lipid mobility. High concentrations of Protein A are required for presenting a high charge density on the surface, leading to a rigid layer with a stable hydration layer that limits the ability of proteins to irreversibly bind. These results underpin the importance of lipid and surface charges in enabling effective antifouling function as they were only effective with a compatible sensor surface. As such, lipid surfaces show incredible promise in enabling sensing of biological targets in complex media but must be properly incorporated into the sensor development process to account for surface charge and binding effects that play a crucial role in the formation and effectiveness of antifouling lipid surfaces.

Supporting Information

FRAP, MALDI-MS spectrum of EPC lipids and SPR sensorgram showing lipid membrane formation with low Protein A concentration.

ACKNOWLEDGMENT

We would like to acknowledge financial support from NSF (CHE-2109042). MALDI-MS spectra were collected at the Analytical Chemistry Instrumentation Facility at the University of California, Riverside.

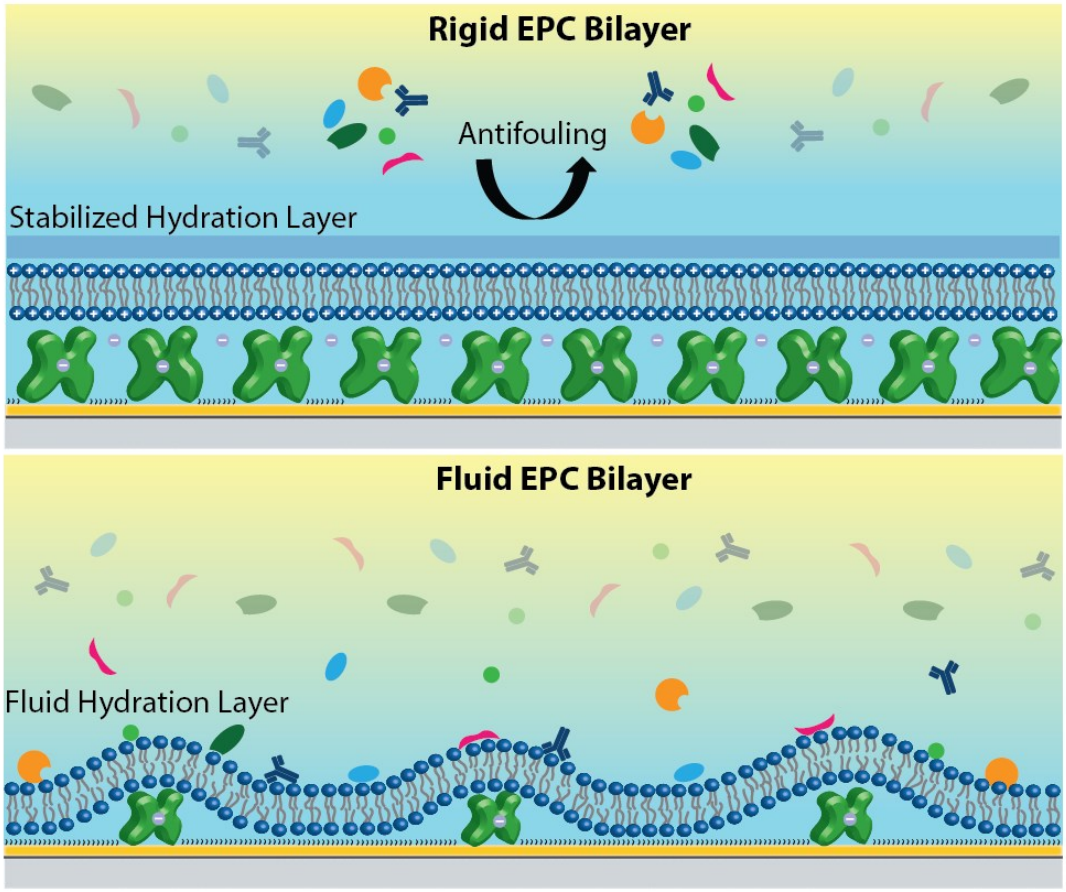

Scheme 1. Antifouling effects of EPC lipid membranes on Protein A scaffolds modulated by surface protein coverage. Rigid EPC bilayers tend to form on high concentration Protein A surface, leading to a highly antifouling surface (top). On low concentration Protein A surfaces, the bilayers are less compact, more mobile, and susceptible to non-specific serum interactions (bottom).

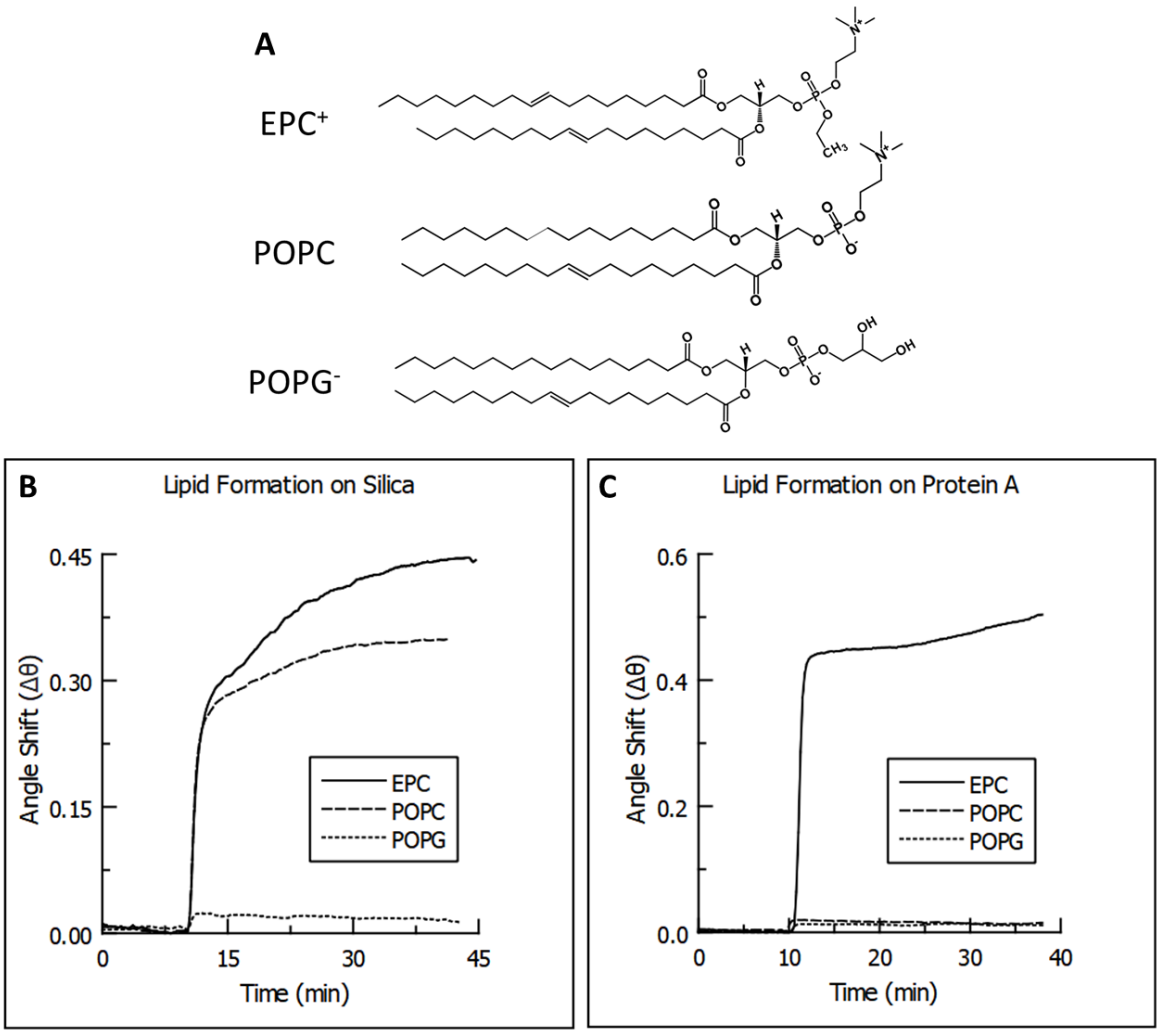

Figure 1. (A) Molecular structure of lipids used in this study (EPC, POPC, and POPG). (B and C) SPR sensorgrams of lipid vesicle adhesion and fusion to form supported lipid bilayer systems on silica (B) and Protein A (C) with EPC, POPC, and POPG.

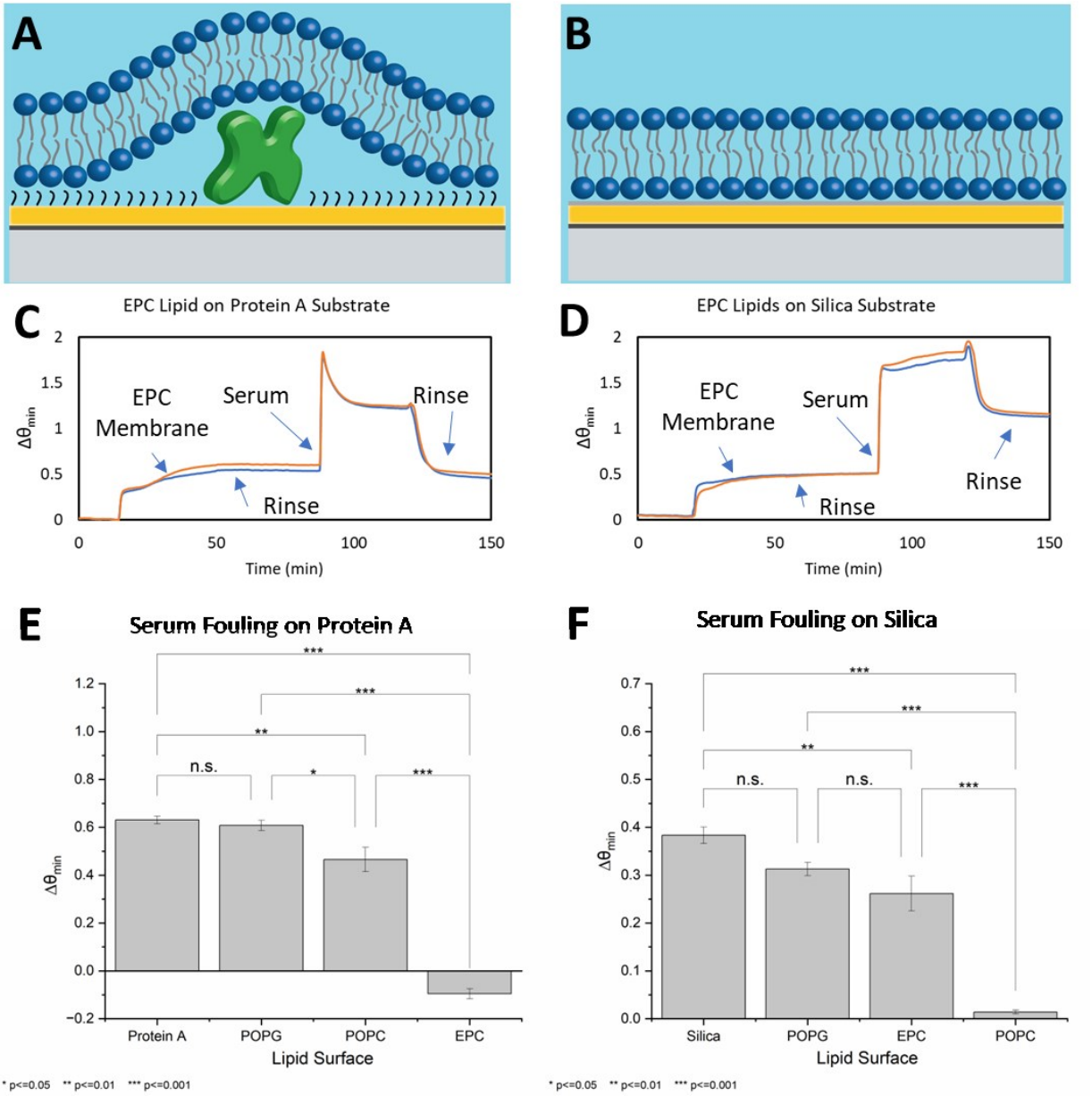

Figure 2. Representation of EPC lipid membranes on Protein A (A) and silica substrates (B). (C) Representative SPR sensorgram showing the antifouling effect of EPC against serum on a Protein A surface. (D) Representative SPR sensorgram showing the antifouling effect on a silica substrate. (E and F) Bar plots showing the SPR results in angular shifts from serum nonspecific interactions on the surfaces of a Protein A formulation (E) (n=5) and on silica (F) (n≥5).

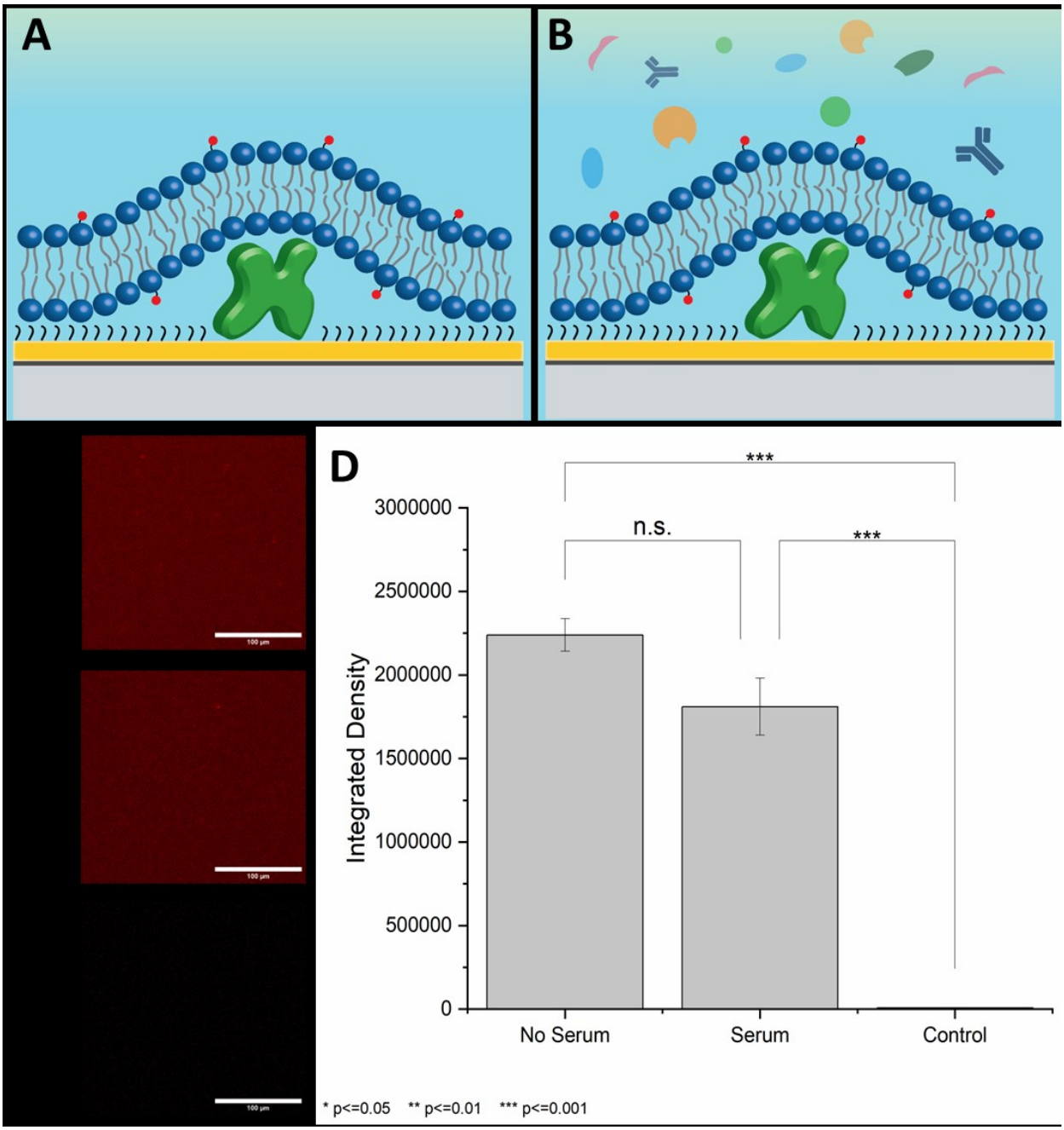

Figure 3. Cartoon representation of fluorescently labeled lipid surface on Protein A without serum introduction (A) and with serum incubation (B). (C) shows fluorescent images of EPC membranes on a Protein A surface before serum introduction (top), after serum incubation (middle), and without fluorophore labeled lipids (bottom, as a control). Scale bars are 100 μm. (D) Bar plot showing the average density of displayed fluorescent images with error bars calculated from triplicate results.

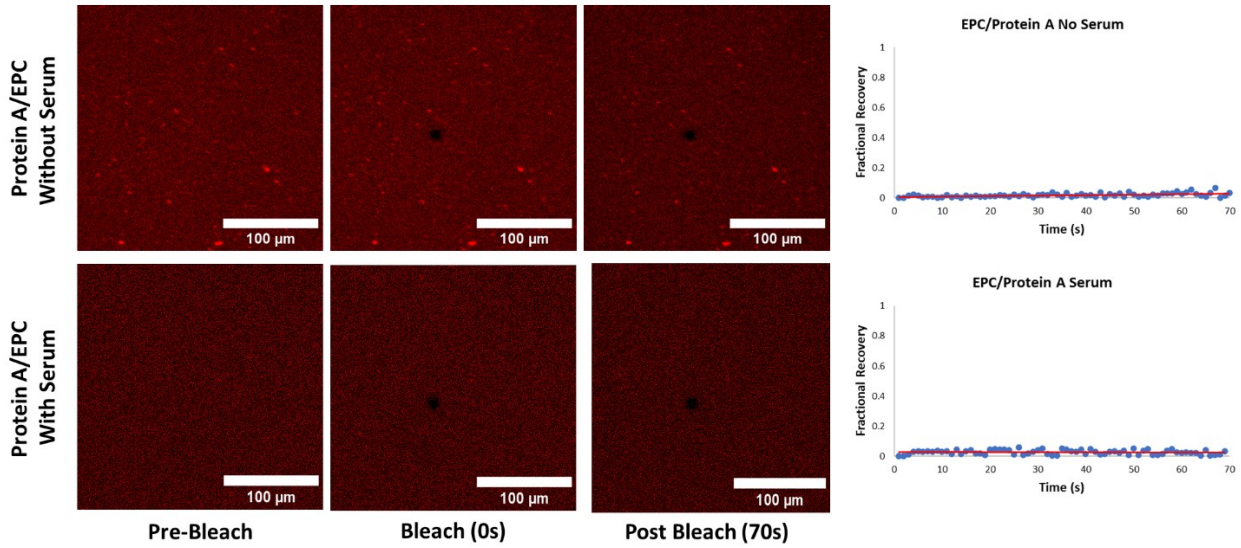

Figure 4. FRAP results displaying EPC membranes on Protein A surfaces before (top) and after (bottom) serum fouling interactions. Time points showing before the bleach (left column), immediately after bleach (middle column), and 70 seconds after bleaching (right column). Scale bars are 100 µm. The resulting fractional recovery rates are displayed on the right.

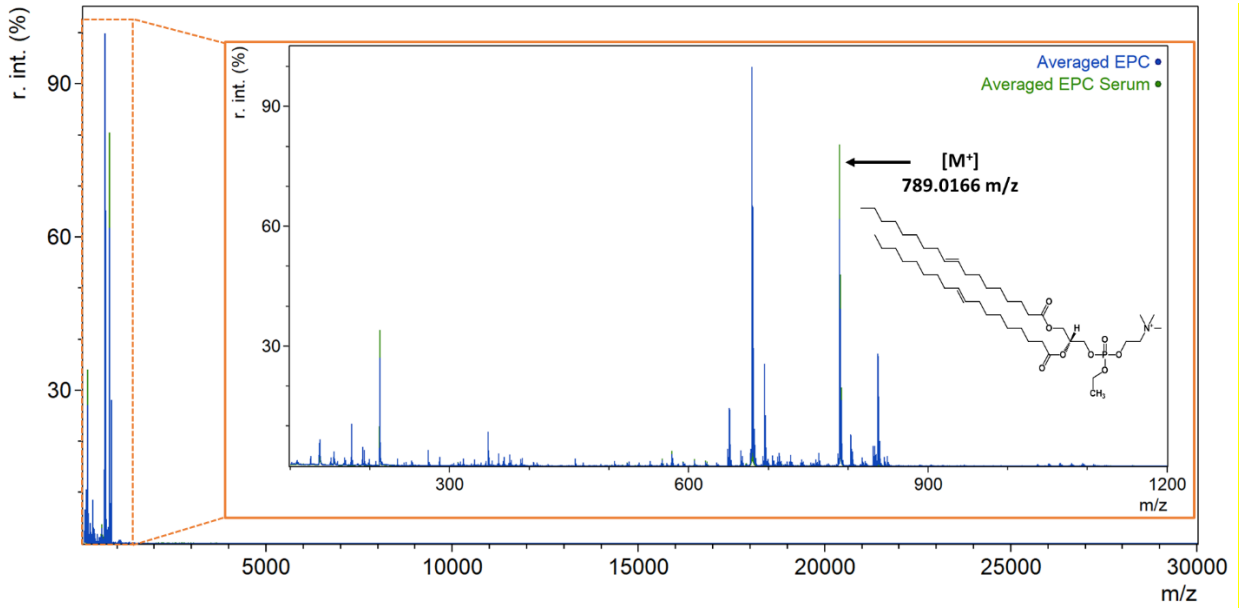

Figure 5. MALDI-MS spectra in positive ion mode for an EPC lipid membrane on a Protein A surface before (blue) and after serum incubation (green). Insert in the orange frame is a blowup for the spectrum in the m/z range of 150-1200. No peaks were identifiable beyond 1200 m/z and EPC lipids were identified at 789.01 m/z as a molecular ion as shown in the inset.

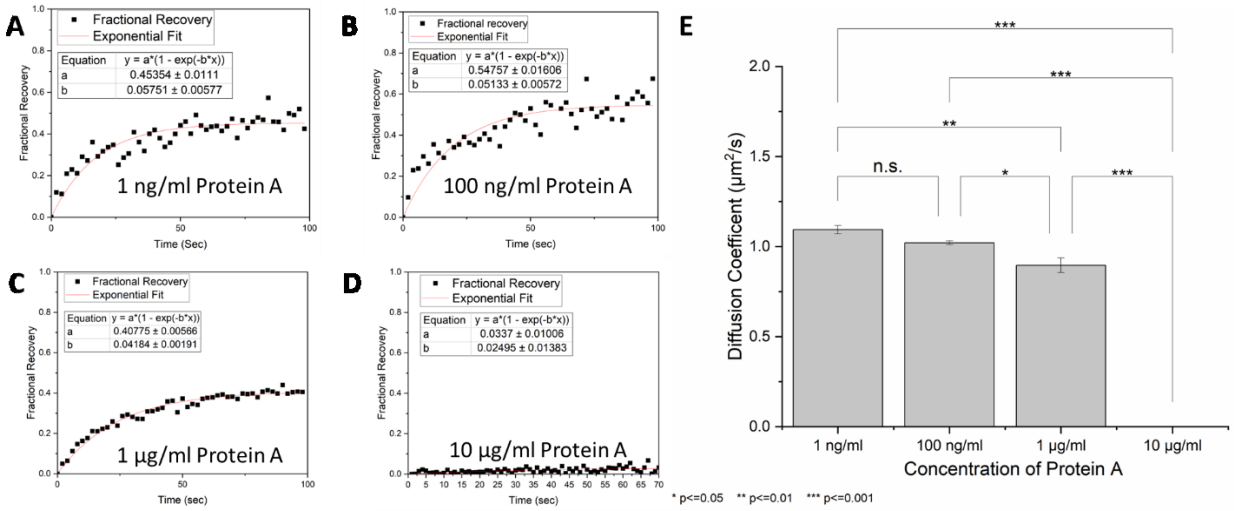

Figure 6. Lipid diffusivity changes due to Protein A concentration. (A-D) Fractional recovery curves and the fits used to calculate lipid diffusivity for EPC lipids on increasing concentrations of Protein A substrates (1ng/ml, 100 ng/ml, 1 µg/ml, and 10 µg/ml, respectively). (E) Calculated diffusion coefficients from FRAP recovery curve fitting.

References

1. Ouyang, M.; Tu, D.; Tong, L.; Sarwar, M.; Bhimaraj, A.; Li, C.; Cote, G. L.; Di Carlo, D., A review of biosensor technologies for blood biomarkers toward monitoring cardiovascular diseases at the point-of-care. *Biosens Bioelectron* **2021,** *171*, 112621.
2. Azzouz, A.; Hejji, L.; Kim, K. H.; Kukkar, D.; Souhail, B.; Bhardwaj, N.; Brown, R. J. C.; Zhang, W., Advances in surface plasmon resonance-based biosensor technologies for cancer biomarker detection. *Biosens Bioelectron* **2022,** *197*, 113767.
3. Frutiger, A.; Tanno, A.; Hwu, S.; Tiefenauer, R. F.; Voros, J.; Nakatsuka, N., Nonspecific Binding-Fundamental Concepts and Consequences for Biosensing Applications. *Chem Rev* **2021,** *121* (13), 8095-8160.
4. McKeating, K. S.; Hinman, S. S.; Rais, N. A.; Zhou, Z.; Cheng, Q., Antifouling Lipid Membranes over Protein A for Orientation-Controlled Immunosensing in Undiluted Serum and Plasma. *ACS Sens* **2019,** *4* (7), 1774-1782.
5. Malinick, A. S.; Lambert, A. S.; Stuart, D. D.; Li, B.; Puente, E.; Cheng, Q., Detection of Multiple Sclerosis Biomarkers in Serum by Ganglioside Microarrays and Surface Plasmon Resonance Imaging. *ACS Sens* **2020,** *5* (11), 3617-3626.
6. Jiang, C.; Wang, G.; Hein, R.; Liu, N.; Luo, X.; Davis, J. J., Antifouling Strategies for Selective In Vitro and In Vivo Sensing. *Chem Rev* **2020,** *120* (8), 3852-3889.
7. D'Agata, R.; Bellassai, N.; Jungbluth, V.; Spoto, G., Recent Advances in Antifouling Materials for Surface Plasmon Resonance Biosensing in Clinical Diagnostics and Food Safety. *Polymers (Basel)* **2021,** *13* (12).
8. Malinick, A. S.; Stuart, D. D.; Lambert, A. S.; Cheng, Q., Surface plasmon resonance imaging (SPRi) in combination with machine learning for microarray analysis of multiple sclerosis biomarkers in whole serum. *Biosensors and Bioelectronics: X* **2022,** *10*.
9. Wang, Y. S.; Yau, S.; Chau, L. K.; Mohamed, A.; Huang, C. J., Functional Biointerfaces Based on Mixed Zwitterionic Self-Assembled Monolayers for Biosensing Applications. *Langmuir* **2019,** *35* (5), 1652-1661.
10. Duanghathaipornsuk, S.; Reaver, N. G. F.; Cameron, B. D.; Kim, D. S., Adsorption Kinetics of Glycated Hemoglobin on Aptamer Microarrays with Antifouling Surface Modification. *Langmuir* **2021,** *37* (15), 4647-4657.
11. Dedisch, S.; Obstals, F.; los Santos Pereira, A.; Bruns, M.; Jakob, F.; Schwaneberg, U.; Rodriguez‐Emmenegger, C., Turning a Killing Mechanism into an Adhesion and Antifouling Advantage. *Advanced Materials Interfaces* **2019,** *6* (18).
12. Nie, W.; Wang, Q.; Zou, L.; Zheng, Y.; Liu, X.; Yang, X.; Wang, K., Low-Fouling Surface Plasmon Resonance Sensor for Highly Sensitive Detection of MicroRNA in a Complex Matrix Based on the DNA Tetrahedron. *Anal Chem* **2018,** *90* (21), 12584-12591.
13. Olivier R. Bolduc, J. N. P., †,‡ and Jean-Franc¸ ois Masson, SPR Biosensing in Crude Serum Using Ultralow Fouling Binary Patterned Peptide SAM. *Analytical Chemistry* **2010,** *82*, 3699–3706.
14. Mao, Z.; Zhao, J.; Chen, J.; Hu, X.; Koh, K.; Chen, H., A simple and direct SPR platform combining three-in-one multifunctional peptides for ultra-sensitive detection of PD-L1 exosomes. *Sensors and Actuators B: Chemical* **2021,** *346*.
15. Sut, T. N.; Yoon, B. K.; Jeon, W.-Y.; Jackman, J. A.; Cho, N.-J., Supported lipid bilayer coatings: Fabrication, bioconjugation, and diagnostic applications. *Applied Materials Today* **2021,** *25*.

16. Jiang, X.; Zhu, Q.; Zhu, H.; Zhu, Z.; Miao, X., Antifouling lipid membrane coupled with silver nanoparticles for electrochemical detection of nucleic acids in biological fluids. *Anal Chim Acta* **2021,** *1177*, 338751.
17. Jackman, J. A.; Cho, N. J., Supported Lipid Bilayer Formation: Beyond Vesicle Fusion. *Langmuir* **2020,** *36* (6), 1387-1400.
18. Luchini, A.; Vitiello, G., Mimicking the Mammalian Plasma Membrane: An Overview of Lipid Membrane Models for Biophysical Studies. *Biomimetics (Basel)* **2020,** *6* (1).
19. Liu, Y.; Chen, D.; Zhang, W.; Zhang, Y., Mobile DNA tetrahedron on ultra-low adsorption lipid membrane for directional control of cell sensing. *Sensors and Actuators B: Chemical* **2020,** *307*.
20. Masson, J. F., Surface Plasmon Resonance Clinical Biosensors for Medical Diagnostics. *ACS Sens* **2017,** *2* (1), 16-30.
21. Baggerman, J.; Smulders, M. M. J.; Zuilhof, H., Romantic Surfaces: A Systematic Overview of Stable, Biospecific, and Antifouling Zwitterionic Surfaces. *Langmuir* **2019,** *35* (5), 1072-1084.
22. Asha, A. B.; Chen, Y.; Narain, R., Bioinspired dopamine and zwitterionic polymers for non-fouling surface engineering. *Chem Soc Rev* **2021,** *50* (20), 11668-11683.
23. Klausen, L. H.; Fuhs, T.; Dong, M., Mapping surface charge density of lipid bilayers by quantitative surface conductivity microscopy. *Nat Commun* **2016,** *7*, 12447.
24. Yeung, T.; Grinstein, S., Lipid signaling and the modulation of surface charge during phagocytosis. *Immunol Rev* **2007,** *219*, 17-36.
25. Lu, S. M.; Fairn, G. D., Mesoscale organization of domains in the plasma membrane - beyond the lipid raft. *Crit Rev Biochem Mol Biol* **2018,** *53* (2), 192-207.
26. Andersson, J.; Bilotto, P.; Mears, L. L. E.; Fossati, S.; Ramach, U.; Köper, I.; Valtiner, M.; Knoll, W., Solid-supported lipid bilayers – A versatile tool for the structural and functional characterization of membrane proteins. *Methods* **2020,** *180*, 56-68.
27. Day, C. A.; Kang, M., The Utility of Fluorescence Recovery after Photobleaching (FRAP) to Study the Plasma Membrane. **2023,** *13* (5), 492.
28. Stuart, D. D.; Ebel, C. P.; Cheng, Q., Biosensing empowered by molecular identification: Advances in surface plasmon resonance techniques coupled with mass spectrometry and Raman spectroscopy. *Sensors and Actuators Reports* **2022,** *4*, 100129.
29. Abbas, A.; Linman, M. J.; Cheng, Q., Patterned resonance plasmonic microarrays for high-performance SPR imaging. *Anal Chem* **2011,** *83* (8), 3147-52.
30. Blumenthal, D.; Goldstien, L.; Edidin, M.; Gheber, L. A., Universal Approach to FRAP Analysis of Arbitrary Bleaching Patterns. *Sci Rep* **2015,** *5*, 11655.
31. D. AXELROD, D. E. K., J. SCHLESSINGER, E. ELSON, and W. W. WEBB, MOBILITY MEASUREMENT BY ANALYSIS OF FLUORESCENCE PHOTOBLEACHING RECOVERY KINETICS. *BIOPHYSICAL JOURNAL* **1976,** *16* (9), 1055–1069.
32. Soumpasis, D. M., Theoretical analysis of fluorescence photobleaching recovery experiments. *Biophys J* **1983,** *41* (1), 95-7.
33. Kurniawan, J.; Ventrici de Souza, J. F.; Dang, A. T.; Liu, G. Y.; Kuhl, T. L., Preparation and Characterization of Solid-Supported Lipid Bilayers Formed by Langmuir-Blodgett Deposition: A Tutorial. *Langmuir* **2018,** *34* (51), 15622-15639.
34. Kozlowski, L. P., IPC 2.0: prediction of isoelectric point and pKa dissociation constants. *Nucleic Acids Res* **2021,** *49* (W1), W285-W292.

35. Phillips, K. S.; Wilkop, T.; Wu, J. J.; Al-Kaysi, R. O.; Cheng, Q., Surface plasmon resonance imaging analysis of protein-receptor binding in supported membrane arrays on gold substrates with calcinated silicate films. *J Am Chem Soc* **2006,** *128* (30), 9590-9591.
36. Ferhan, A. R.; Jackman, J. A.; Cho, N. J., Probing Spatial Proximity of Supported Lipid Bilayers to Silica Surfaces by Localized Surface Plasmon Resonance Sensing. *Anal Chem* **2017,** *89* (7), 4301-4308.
37. Anderson, T. H.; Min, Y.; Weirich, K. L.; Zeng, H.; Fygenson, D.; Israelachvili, J. N., Formation of supported bilayers on silica substrates. *Langmuir* **2009,** *25* (12), 6997-7005.
38. Li, H.; Dauphin-Ducharme, P.; Arroyo-Curras, N.; Tran, C. H.; Vieira, P. A.; Li, S.; Shin, C.; Somerson, J.; Kippin, T. E.; Plaxco, K. W., A Biomimetic Phosphatidylcholine-Terminated Monolayer Greatly Improves the In Vivo Performance of Electrochemical Aptamer-Based Sensors. *Angew Chem Int Ed Engl* **2017,** *56* (26), 7492-7495.
39. Cho, N. J.; Frank, C. W.; Kasemo, B.; Hook, F., Quartz crystal microbalance with dissipation monitoring of supported lipid bilayers on various substrates. *Nat Protoc* **2010,** *5* (6), 1096-106.
40. Tamm, L. K.; Mcconnell, H. M., Supported Phospholipid-Bilayers. *Biophysical Journal* **1985,** *47* (1), 105-113.
41. Su, Q.; Jiang, C.; Gou, D.; Long, Y., Surface Plasmon-Assisted Fluorescence Enhancing and Quenching: From Theory to Application. *ACS Appl Bio Mater* **2021,** *4* (6), 4684-4705.
42. Farell, M.; Wetherington, M.; Shankla, M.; Chae, I.; Subramanian, S.; Kim, S. H.; Aksimentiev, A.; Robinson, J.; Kumar, M., Characterization of the Lipid Structure and Fluidity of Lipid Membranes on Epitaxial Graphene and Their Correlation to Graphene Features. *Langmuir* **2019,** *35* (13), 4726-4735.
43. Cho, N. J.; Cho, S. J.; Cheong, K. H.; Glenn, J. S.; Frank, C. W., Employing an amphipathic viral peptide to create a lipid bilayer on Au and TiO2. *J Am Chem Soc* **2007,** *129* (33), 10050-1.
44. Tabaei, S. R.; Choi, J. H.; Haw Zan, G.; Zhdanov, V. P.; Cho, N. J., Solvent-assisted lipid bilayer formation on silicon dioxide and gold. *Langmuir* **2014,** *30* (34), 10363-73.
45. Hosseini, S., Martinez-Chapa, S.O., Principles and Mechanism of MALDI-ToF-MS Analysis. In: Fundamentals of MALDI-ToF-MS Analysis. *SpringerBriefs in Applied Sciences and Technology* **2017**, 1-19.
46. Roach, P.; Farrar, D.; Perry, C. C., Interpretation of protein adsorption: Surface-induced conformational changes. *J Am Chem Soc* **2005,** *127* (22), 8168-8173.
47. Lambert, A. S.; Valiulis, S. N.; Malinick, A. S.; Tanabe, I.; Cheng, Q., Plasmonic Biosensing with Aluminum Thin Films under the Kretschmann Configuration. *Anal Chem* **2020,** *92* (13), 8654-8659.
48. Jackman, J. A.; Tabaei, S. R.; Zhao, Z.; Yorulmaz, S.; Cho, N. J., Self-assembly formation of lipid bilayer coatings on bare aluminum oxide: overcoming the force of interfacial water. *ACS Appl Mater Interfaces* **2015,** *7* (1), 959-68.
49. van Weerd, J.; Karperien, M.; Jonkheijm, P., Supported Lipid Bilayers for the Generation of Dynamic Cell-Material Interfaces. *Adv Healthc Mater* **2015,** *4* (18), 2743-79.
50. Marta Pasenkiewicz-Gierula, Y. T., Hiroo Miyagawa, Kunihiro Kitamura, and Akihiro Kusum, Hydrogen Bonding of Water to Phosphatidylcholine in the Membrane As Studied by a Molecular Dynamics Simulation: Location, Geometry, and Lipid-Lipid Bridging via Hydrogen-Bonded Water. *J. Phys. Chem. A* **1997,** *101*, 3677-3691.

51. Qiao, X.; Qian, Z. H.; Sun, W.; Zhu, C. Y.; Li, Y.; Luo, X., Phosphorylation of Oligopeptides: Design of Ultra-Hydrophilic Zwitterionic Peptides for Anti-Fouling Detection of Nucleic Acids in Saliva. *Anal Chem* **2023**.

Graphic content